Vol.2011-CG-145 No.21
Vol.2011-CVIM-179 No.21
2011/11/18

Automatic Radiometric Calibration in Photometric Stereo by Using Irradiance Consistency

Wiennat Mongkulmann ,[†1] Takahiro Okabe [†1]
and Yoichi Sato[†1]

We propose a method for estimating the surface normals and camera response function simultaneously. In photometric stereo, camera is assumed to be radiometrically calibrated then the observed pixel intensity can be used to subsume the image irradiance. Our proposed method shows that such often time-consuming radiometric calibration can be avoided, while the camera response function and surface normals can be estimated at the same time. The key idea of our method is that the irradiance values converted from pixel values by radiometric response function must be equal to corresponding irradiance values calculated from the surface normals. We show that the simultaneous estimation can be expressed as a linear least-square problem with linear constraint. Finally, experiments on both synthetic images and real images demonstrate that our method can accurately estimate surface normals even when the images are captured by using uncalibrated camera with nonlinear radiometric response function.

1. Introduction

Photometric stereo is a technique for estimating surface orientations from a set of images of a stationary object taken from a fixed viewpoint and under different light sources. Since Woodham[1)] first addressed photometric stereo under the assumptions of the Lambert model and known light sources, its generalization has extensively been studied. One direction of study is generalization to the case of non-Lambertian reflectance properties, and the other is generalization to the case of unknown light sources.

Another important (but usually implicit) assumption of photometric stereo is that a radiometric response function of a camera is linear, *i.e.* a pixel value is proportional to an image irradiance value. Unfortunately, however, it is well known that consumer cameras generally have nonlinear radiometric response functions[2)]. Therefore, photometric stereo requires cumbersome calibration of a radiometric response function in advance, so that image irradiance values can be determined from observed pixel values. This would be one of the main reasons that photometric stereo is not necessarily used widely out of the computer vision community.

In this paper, we propose a novel method that avoids this radiometric calibration preprocessing from photometric stereo; our proposed method simultaneously estimates surface normals and an inverse radiometric response function, which maps a pixel value to an image irradiance value. The key idea of our method is to make use of the consistency between an inverse radiometric response function and surface normals; the irradiance values converted from pixel values by using the inverse radiometric response function should be equal to the corresponding irradiance values calculated from the surface normals. In other words, we take advantage of such a clue, which is inherent in the physical model of reflectance itself, for estimating surface normals as well as an inverse radiometric response function.

Specifically, our proposed method represents an inverse radiometric response function as a linear combination of polynomials with respect to pixel values in a similar manner to Mitsunaga and Nayar[2)], and then estimates surface normals and the coefficients of the polynomials at the same time. We show that the simultaneous estimation results in a linear least-square problem with linear constraints. Here, the former comes from the consistency between two irradiance values: one is from the inverse radiometric response function and the other is from the surface normals, and the latter stems from the monotonicity of the inverse radiometric response function. We demonstrate that our method can accurately estimate both surface normals and a radiometric response function via a number of experiments using synthetic and real images.

The main contribution of this study is to achieve photometric stereo with auto-radiometric calibration. Therefore, our method requires neither cumbersome calibration of a radiometric response function nor additional images used for radiometric calibration. Our proposed framework enables us to use photometric stereo without worrying about a radiometric response function of a camera.

†1 Institute of Industrial Science, The University of Tokyo

The rest of this paper is organized as follows. We briefly summarize related work in Section 2. A method for simultaneously estimating surface normals and an inverse radiometric response function is proposed in Section 3. We present the experimental results in Section 4 and concluding remarks in Section 5.

2. Related Work

There are several methods for estimating a radiometric response function of a camera. One of the most widely used methods is the pioneering work by Mitsunaga and Nayar[2]. They conduct radiometric calibration by using multiple images of a static scene taken with different exposure times. After that, Lin *et al.*[3),4)] proposed a method for estimating a radiometric response function from a single color/grayscale image. Their method is based on color/intensity mixtures along edge boundaries, *i.e.* spatial irradiance mixtures. Wilburn *et al.*[5)] conduct radiometric calibration on the basis of motion blur in a single image. They make use of temporal irradiance mixtures instead of spatial ones. Kim and Pollefeys[6)] estimate a radiometric response function from an image sequence taken with a moving camera by computing pixel correspondences across the image frames. Grossberg and Nayar[7)] show that radiometric calibration can be done by using the intensity histograms of two image frames without exact registration. Recently, Lee *et al.*[8)] formulate the radiometric calibration from multiple images with different exposure times as a rank minimization problem, and achieve better performance than existing techniques.

We can conduct radiometric calibration by using those existing techniques as a completely independent preprocessing. However, those techniques are often cumbersome and usually require additional images used for radiometric calibration. Unlike those techniques, our proposed method does not require additional images. More importantly, our method is based on a different clue; we take advantage of the physical model of reflectance for radiometric calibration.

Our proposed method is similar in spirit to Shi *et al.*[9)]. Interestingly, they investigate a color profile, *i.e.* the set of RGB values at a certain pixel under different light sources, and demonstrate that input images to photometric stereo can be used also for radiometric calibration. Their method is based on the observation that a color profile draws a straight line (curve) in RGB space when a radiometric response function is linear (nonlinear). Therefore, they estimate a radiometric response function so that the color profiles are linearized. Although their method does not require additional images for radiometric calibration, it is still considered as a preprocessing, and requires nonlinear optimization and color images. More importantly, their method cannot handle a certain class of radiometric response functions such as a polynomial and gray objects for which the color profiles remain straight lines even when a radiometric response function is nonlinear.

On the other hand, as far as we know, ours is the only method that can estimate surface normals and a radiometric response function simultaneously. In addition, our method does not require nonlinear optimization and color images, and can handle polynomial response functions and gray objects.

3. Proposed Method

3.1 Photometric Stereo

We briefly summarize the classic photometric stereo[1)] which assumes the Lambert model, known light sources, and a linear radiometric response function.

Let us denote the irradiance at the p-th surface point ($p = 1, 2, ..., P$) under the l-th light source ($l = 1, 2, ..., L$) by I_{pl}. Assuming the Lambert model, the irradiance I_{pl} is described as

$$I_{pl} = \boldsymbol{n}_p^T \boldsymbol{l}_l, \tag{1}$$

where $\boldsymbol{n}_p$ is the surface normal at the p-th surface point scaled by its albedo and $\boldsymbol{l}_l$ is the direction of the l-th light source scaled by its intensity.

The classic photometric stereo estimates the scaled surface normal $\boldsymbol{n}_p$ from the irradiances I_{pl} ($l = 1, 2, ..., L$) assuming that the scaled light source directions $\boldsymbol{l}_l$ ($l = 1, 2, ..., L$) are known. Since the scaled surface normal $\boldsymbol{n}_p$ has three degrees of freedom, *i.e.* two for the surface normal vector with unit length and one for the albedo, we can estimate the surface normal from three images at least ($L \geq 3$).

Conventionally, eq.(1) is described in the matrix form:

$$\begin{pmatrix} I_{p1} \\ \vdots \\ I_{pL} \end{pmatrix} = \begin{pmatrix} l_{1x} & l_{1y} & l_{1z} \\ \vdots & \vdots & \vdots \\ l_{Lx} & l_{Ly} & l_{Lz} \end{pmatrix} \begin{pmatrix} n_{px} \\ n_{py} \\ n_{pz} \end{pmatrix},$$

$$\boldsymbol{I}_p = \boldsymbol{L}\boldsymbol{n}_p, \tag{2}$$

where $\boldsymbol{l}_l = (l_{lx}, l_{ly}, l_{lz})^T$ and $\boldsymbol{n}_p = (n_{px}, n_{py}, n_{pz})^T$. The estimate of the scaled surface normal $\hat{\boldsymbol{n}}_p$ is given by the least-square method:

$$\hat{\boldsymbol{n}}_p = \left(\boldsymbol{L}^T\boldsymbol{L}\right)^{-1}\boldsymbol{L}^T\boldsymbol{I}_p. \tag{3}$$

This is equivalent to

$$\hat{\boldsymbol{n}}_p = \arg\min_{\boldsymbol{n}_p} \sum_{l=1}^{L} \left(I_{pl} - \boldsymbol{n}_p^T\boldsymbol{l}_l\right)^2. \tag{4}$$

The surface normal and albedo are computed from the estimated scaled surface normal $\hat{\boldsymbol{n}}_p$ as $\hat{\boldsymbol{n}}_p/|\hat{\boldsymbol{n}}_p|$ and $|\hat{\boldsymbol{n}}_p|$ respectively.

3.2 Radiometric Response Function

The radiometric response function f maps an irradiance value I to a pixel value I'. Since the radiometric response function is a monotonically increasing function, there is a unique inverse function $g = f^{-1}$ which maps a pixel value I' to an irradiance value I. Hereafter, we normalize the ranges of pixel values and irradiance values to $[0, 1]$ without loss of generality.

In a similar manner to the existing technique[2], we represent the inverse radiometric response function by using polynomials:

$$I = g(I') = \sum_{k=0}^{K} c_k I'^k, \tag{5}$$

where c_k is the coefficient of the k-th polynomial.

Since the inverse radiometric response function g is also a monotonically increasing function with respect to a pixel value I', the coefficients $\{c_k\}$ satisfy the monotonicity constraint:

$$\frac{dg(I')}{dI'} = \sum_{k=1}^{K} k c_k I'^{k-1} > 0, \tag{6}$$

when $I' > 0$. In addition, since the ranges of pixel values and irradiance values are normalized, the coefficients $\{c_k\}$ satisfy the boundary conditions:

$$g(0) = c_0 = 0, \quad g(1) = \sum_{k=0}^{K} c_k = 1. \tag{7}$$

3.3 Simultaneous Estimation

Our proposed method estimates both the surface normals $\boldsymbol{n}_p$ $(p = 1, 2, ..., P)$ and the coefficients of the inverse radiometric response function c_k $(k = 1, 2, ..., K)$ at the same time.

Substituting eq.(7) into eq.(5) and eliminating c_1, an irradiance I is described by using a pixel value I' as

$$\begin{aligned} I &= c_1 I' + \sum_{k=2}^{K} c_k I'^k \\ &= I' + \sum_{k=2}^{K} c_k \left(I'^k - I'\right). \end{aligned} \tag{8}$$

Therefore, in a similar manner to eq.(4), the estimates of the surface normals $\{\hat{\boldsymbol{n}}_p\}$ and the coefficients of the inverse radiometric response function $\{\hat{c}_k\}$ are given by

$$\begin{aligned} &(\{\hat{\boldsymbol{n}}_p\}, \{\hat{c}_k\}) = \arg \min_{(\{\boldsymbol{n}_p\}, \{c_k\})} \\ &\sum_{p=1}^{P}\sum_{l=1}^{L} \left[I'_{pl} - \boldsymbol{n}_p^T\boldsymbol{l}_l + \sum_{k=2}^{K} c_k \left(I'^k_{pl} - I'_{pl}\right) \right]^2. \end{aligned} \tag{9}$$

Here, the third term in the bracket acts as a correction term for compensating a nonlinear radiometric response function.

As to the monotonicity constraint, substituting eq.(7) into eq.(6), we obtain

$$\sum_{k=2}^{K} c_k (1 - k I'^{k-1}) > 1. \tag{10}$$

Therefore, the coefficients have to satisfy this inequality for arbitrary pixel values, *e.g.* $I' = i/255$ $(i = 1, 2, ..., 254)$ for 8 bit images.

Thus, the simultaneous estimation of the surface normals and the inverse radiometric response function results in the linear least-square problem in eq.(9) with the linear constraints in eq.(10). Since this problem is a convex quadratic

Vol.2011-CG-145 No.21
Vol.2011-CVIM-179 No.21
2011/11/18

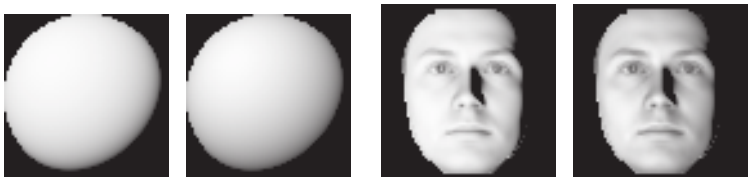

Fig. 1 Synthetic images of sphere and face with different radiometric response functions.

programming, we can find the globally optimal solution if the number of observations (LP) is larger than the number of unknowns ($3P + K$). Suppose that the number of pixels P is larger than the number of polynomials K, we can estimate the surface normals and the inverse radiometric response function from four images at least ($L \geq 3 + K/P$).

When the radiometric response function is linear, we can estimate a surface normal at each surface point independently as shown in eq.(4). On the other hand, when it is nonlinear, we cannot deal with each surface point independently as shown in eq.(9). Therefore, the naive optimization of eq.(9) subject to the constraints of eq.(10) is computationally expensive when the number of pixels increases. To reduce the computational cost, we can estimate the inverse radiometric response function (and the surface normals) by using a small number of randomly sampled pixels, and then convert pixel values to irradiance values, and finally estimate the surface normals by using eq.(4). Although we did not mention for the sake of simplicity, we detect outliers, *i.e.* shadowed or saturated pixels by using thresholds and remove them from the summations in eq.(4) and eq.(9).

4. Experiments

We used MATLAB implementation of the trust region reflective quadratic programming for optimization. The whole process took about 2.5 seconds for synthetic images and about 7.5 seconds for real images on average by using an Intel Core i7-2600 3.4GHz CPU.

4.1 Synthetic Images

We compared the performance of our proposed method with that of the classic photometric stereo[1)] by using synthetic images. The target objects are a sphere with uniform albedo and a face with relatively complex shape and non-uniform albedo shown in Figure 1. The number of images is 16, and the numbers of foreground pixels of the sphere and face are 3228 and 2776 respectively. We used two radiometric response functions: one is the Agfapan APX 400CD and the other is the polynomial $f = I^{0.4}$. We empirically set the number of polynomials in eq.(5) as $K = 6$.

In Figure 2, we show the qualitative results for the sphere. We show the

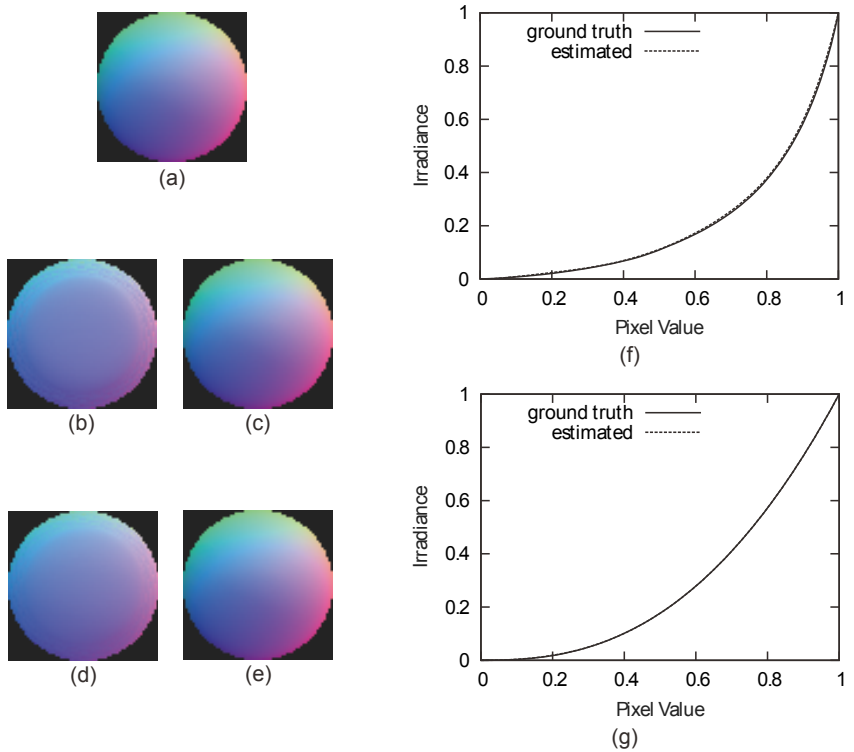

Fig. 2 Results using synthetic images: sphere. (a) the ground truth, (b) the estimated surface normals by using the classic photometric stereo, (c) the estimated ones by using our proposed method, and (f) the inverse radiometric response functions: the solid line stands for the ground truth and the dashed line stands for the estimated one. (d), (e), and (g) are the results for images with the other radiometric response function.

Vol.2011-CG-145 No.21
Vol.2011-CVIM-179 No.21
2011/11/18

Table 1 Average errors of estimated surface normals and RMS errors of estimated inverse radiometric response functions: synthetic images.

	Surface normal (classic)	Surface normal (ours)	Inverse response function
Sphere(Agfapan)	23.6°	1.6°	0.0056
Sphere(polynomial)	18.7°	1.9°	0.0004
Face(Agfapan)	17.8°	1.7°	0.0068
Face(polynomial)	15.1°	1.7°	0.0004

color coded surface normals[⋆1]: (a) the ground truth, (b) the estimated ones by using the classic photometric stereo, (c) the estimated ones by using our proposed method, and (f) the inverse radiometric response functions: the solid line stands for the ground truth and the dashed line stands for the estimated one. One can see that the estimated surface normals by using our method looks similar to the ground truth while the estimated surface normals by using the classic photometric stereo are significantly distorted. Moreover, one can see that the estimated inverse radiometric response function is almost the same as the ground truth. We show the results for images with the other radiometric response function in (d), (e), and (g). One can see that those results are consistent with (b), (c), and (f).

In Figure 3, we show the qualitative results for the face. Similar to the experimental results for the sphere, one can see that the estimated surface normals by using our proposed method, *i.e.* (c) and (e) are clearly better than the estimated surface normals by using the classic photometric stereo, *i.e.* (b) and (d). In addition, one can see that the estimated inverse radiometric response functions are almost the same as the ground truths.

Table 1 shows the quantitative results: the average errors of the estimated surface normals and the RMS errors of the estimated inverse radiometric response functions. One can see that the average errors of the estimated surface normals are drastically decreased by simultaneously estimating surface normals and a radiometric response function. Moreover, one can see that our proposed method can accurately estimate the inverse radiometric response functions as a by-product.

⋆1 x, y, and z components ($\in [-1, 1]$) are linearly mapped to RGB.

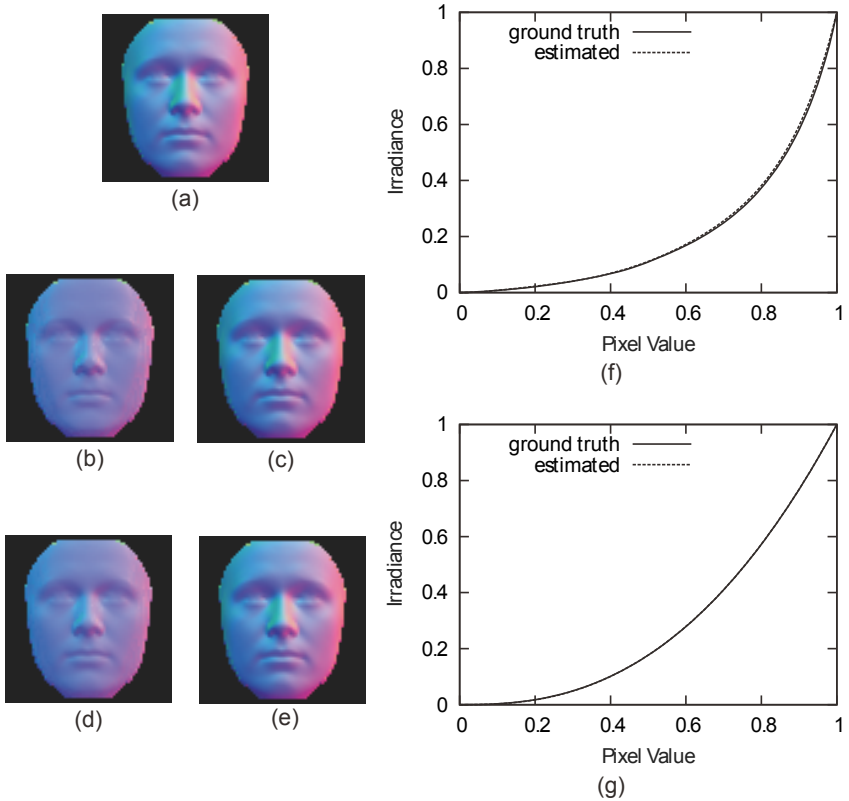

Fig. 3 Results using synthetic images: face.

4.2 Real Images

We compared the performance of our proposed method with that of the classic photometric stereo by using real images. The target objects are a sphere and a statue shown in Figure 4. We captured 10 images by using a Point Grey Chameleon camera with different gamma settings: $g = I'^{2.0}$ and $g = I'^{0.5}$. The numbers of foreground pixels of the sphere and statue are 7063 and 23115 respectively. We computed the ground truth for the surface normals of the sphere on the basis of its silhouette image. As to the statue, we considered the surface

Vol.2011-CG-145 No.21
Vol.2011-CVIM-179 No.21
2011/11/18

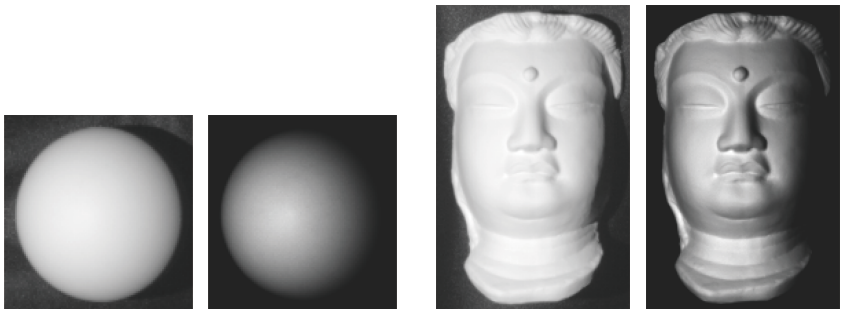

Fig. 4 Real images of sphere and statue with different radiometric response functions.

Table 2 Average errors of estimated surface normals and RMS errors of estimated inverse radiometric response functions: real images.

	Surface normal (classic)	Surface normal (ours)	Inverse response function
Sphere(2.0)	11.3°	2.3°	0.027
Sphere(0.5)	13.1°	3.1°	0.015
Statue(2.0)	11.6°	2.1°	0,021
Statue(0.5)	13.0°	2.6°	0.015

normals estimated by using the classic photometric stereo from images with a linear response function as the ground truth.

In Figure 5 and Figure 6, we show the qualitative results for the sphere and the statue. Similar to the experimental results using synthetic images, one can see that the estimated surface normals by using our proposed method, *i.e.* (c) and (e) are better than the estimated surface normals by using the classic photometric stereo, *i.e.* (b) and (d). In addition, one can see that the estimated inverse radiometric response function (the dashed line) is close to the ground truth (the solid line). Here, we plot the estimated radiometric response function within the range which covers observed pixel values. The estimated radiometric response function is not necessarily accurate out of the range because there is no observation.

Table 2 shows the quantitative results: the average errors of the estimated surface normals and the RMS errors of the estimated inverse radiometric response

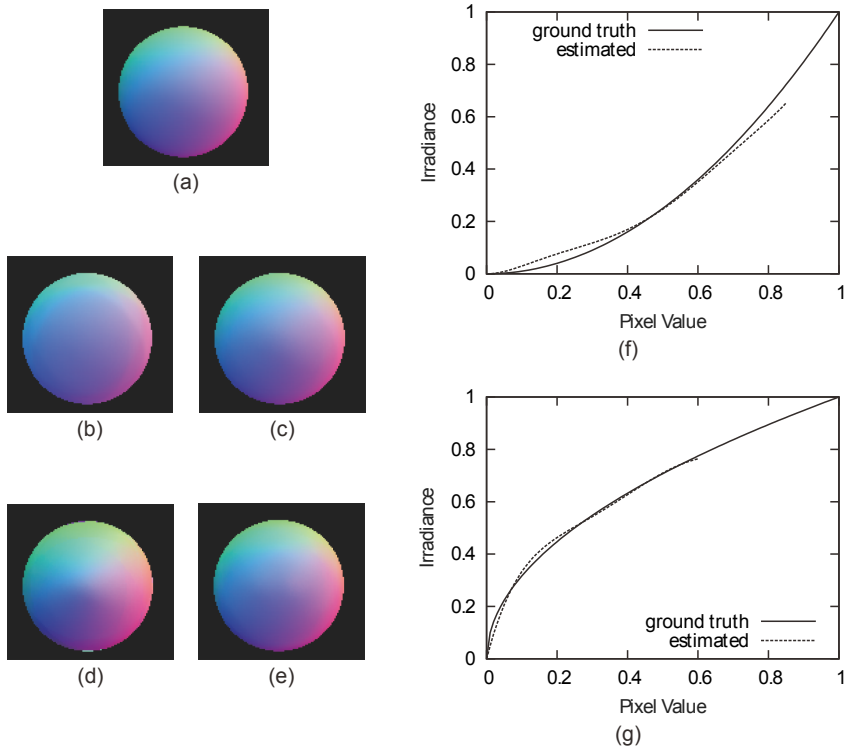

Fig. 5 Results using real images: sphere.

functions. Similar to the experimental results using synthetic images, one can see that the average errors of the estimated surface normals are decreased by simultaneously estimating surface normals and a radiometric response function. Moreover, one can see that our proposed method can accurately estimate the inverse radiometric response functions.

5. Conclusion and Future Work

We presented a novel method for estimating surface normals and a radiometric response function of a camera at the same time. Our proposed method takes advantage of the consistency between the irradiance values from an inverse ra-

Vol.2011-CG-145 No.21
Vol.2011-CVIM-179 No.21
2011/11/18

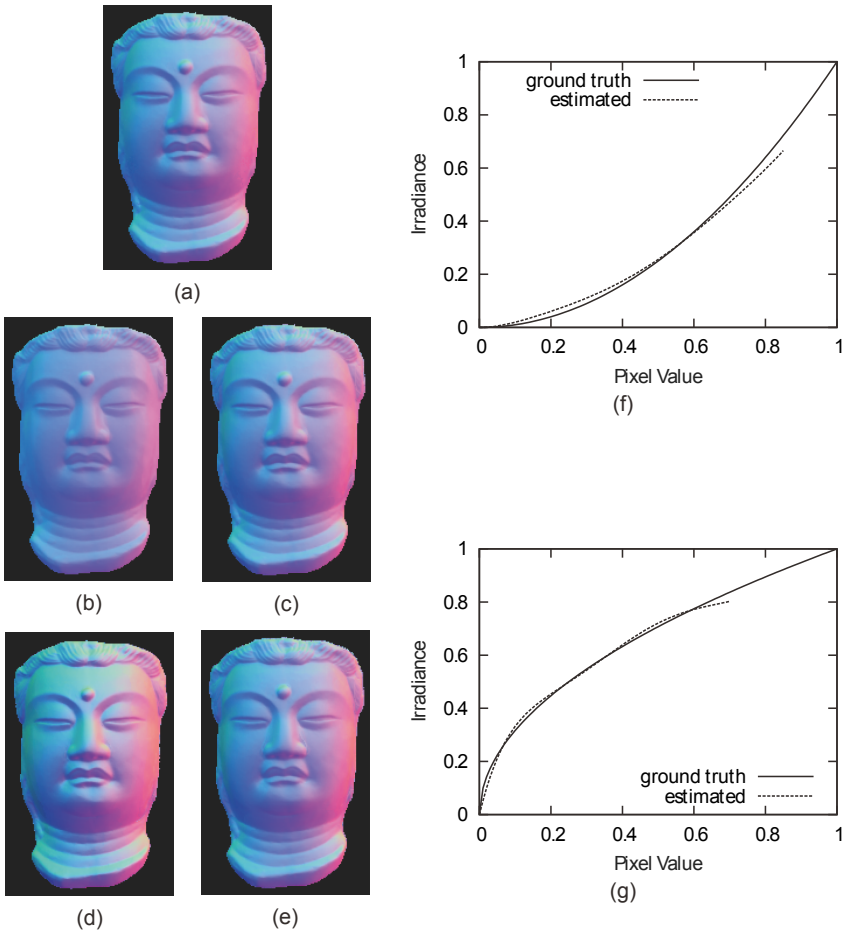

Fig. 6 Results using real images: statue.

diometric response function and those from surface normals, and requires neither cumbersome radiometric calibration preprocessing nor additional images. We demonstrate experimentally that our method can estimate surface normals accurately even when images are captured by using cameras with nonlinear radiometric response functions.

The following issues still remain to be addressed: how to determine the number of polynomials for representing inverse radiometric response functions, and how to sample pixels for reducing computational cost while maintaining the accuracy of the estimated surface normals and radiometric response function. In addition, future work includes the extension of our proposed framework to non-Lambertian reflectance properties and unknown light sources.

Acknowledgment

A part of this work was supported by Grants-in-Aid for Scientific Research from the Ministry of Education, Culture, Sports, Science and Technology of Japan (No. 22680015).

References

1) Woodham, R.: Photometric method for determining surface orientation from multiple images, *Optical Engineering*, Vol.19, No.1, pp.139–144 (1980).
2) Mitsunaga, T. and Nayar, S.: Radiometric self calibration, *Proc. CVPR '99*, pp. 374–380 (1999).
3) Lin, S., Gu, J., Yamazaki, S. and Shum, H.-Y.: Radiometric calibration from a single image, *Proc. CVPR2004*, pp.II–938–II–945 (2004).
4) Lin, S. and Zhang, L.: Determining the radiometric response function from a single grayscale image, *Proc. CVPR2005*, pp.II–66–II–73 (2005).
5) Wilburn, B., Xu, H. and Matsushita, Y.: Radiometric calibration using temporal irradiance mixtures, *Proc. CVPR2008*, pp.1–7 (2008).
6) Kim, S. and Pollefeys, M.: Radiometric alignment of image sequences, *Proc. CVPR2004*, pp.I–645–I–651 (2004).
7) Grossberg, M. and Nayar, S.: Determining the camera response from images: what is knowable?, *IEEE Trans. PAMI*, Vol.25, No.11, pp.1455–1467 (2003).
8) Lee, J.-Y., Shi, B., Matsushita, Y., Kweon, I.-S. and Ikeuchi, K.: Radiometric calibration by transform invariant low-rank structure, *Proc. CVPR2011*, pp.2337–2344 (2011).
9) Shi, B., Matsushita, Y., Wei, Y., Xu, C. and Tan, P.: Self-calibrating photometric stereo, *Proc. CVPR2010*, pp.pp.1118–1125 (2010).